Chinese Chemical Letters 35 (2024) 109737

Contents lists available at ScienceDirect

Chinese Chemical Letters

journal homepage: www.elsevier.com/locate/cclet

Improving gene transfection efficiency of highly branched poly(β-amino ester)s through the *in-situ* conversion of inactive terminal groups

Zhili Li[a,b], Qijun Wo[c,d], Dongdong Huang[e], Dezhong Zhou[b,*], Lei Guo[e,*], Yeqing Mao[a,*]

[a] *Department of Urology, The First Affiliated Hospital, College of Medicine, Zhejiang University, Hangzhou 310000, China*
[b] *School of Chemical Engineering and Technology, Xi'an Jiaotong University, Xi'an 710049, China*
[c] *Urology & Nephrology Center, Department of Urology, Zhejiang Provincial People's Hospital (Affiliated People's Hospital), Hangzhou Medical College, Hangzhou 310014, China*
[d] *Key Laboratory of Endocrine Gland Diseases of Zhejiang Province, Hangzhou 310014, China*
[e] *Pooling Institute of Translational Medicine, Hangzhou 311100, China*

ARTICLE INFO

Article history:
Received 30 November 2023
Revised 16 February 2024
Accepted 21 February 2024
Available online 6 March 2024

Keywords:
Gene therapy
Gene delivery vector
Highly branched poly(β-amino ester)s
Terminal groups
Epithelial cells

ABSTRACT

Highly branched poly(β-amino ester)s (HPAEs) have emerged as a safe and efficient type of non-viral gene delivery vectors. However, the presence of inactive terminal secondary amine groups compromises their gene transfection capability. In this study, HPAEs with similar topological structures and chemical compositions but varying numbers of terminal secondary 4-amino-1-butanol (S4) and secondary/tertiary 3-morpholinopropylamine (MPA) groups were synthesized. The results demonstrate that an increased number of secondary/tertiary MPA groups *in-situ* significantly enhances the DNA binding capability of HPAEs, leading to the formation of smaller HPAE/DNA polyplexes with higher zeta potential, ultimately resulting in superior gene transfection efficiency in bladder epithelial cells. This study establishes a simple yet effective strategy to maximize the gene transfection potency of HPAEs by converting the inactive terminal groups *in-situ* without the need for complex modifications to their topological structure and chemical composition.

With the completion of the Human Genome Project and more disease-related genes are identified, gene therapy has emerged as a potent treatment for various inherited genetic diseases and acquired disorders [1–4]. However, the direct administration of naked nucleic acids is generally inefficient due to multiple extracellular and intracellular biological barriers [5–9]. In contrast, gene delivery vectors can effectively condense or encapsulate nucleic acids into nanoparticles with a positive surface charge, protecting them from enzymatic degradation and facilitating uptake by targeted cells, ultimately improving gene transfection efficiency [10–13].

Gene delivery vectors can be broadly classified into viral vectors and non-viral counterparts. Viral vectors are highly efficient but associated with potential risks related to genomic insertion [14]. Non-viral vectors, on the other hand, have gained attention due to their relatively higher safety and cost-effectiveness, although they are generally less efficient than viral vectors [15]. Among various non-viral gene delivery vectors, poly(β-amino ester)s (PAEs) have shown great potential [16–19]. PAEs can be synthesized through the conjugate addition of amines to acrylates under mild reaction conditions. The availability of diverse monomers allows easy modulation of the chemical composition and properties of PAEs. Initially, linear PAEs (LPAEs) were developed by Lynn and Langer in 2000 [20]. Since then, over 2500 LPAEs have been synthesized and screened for gene transfection using high-throughput technology [21,22].

Considering that a three-dimensional (3D) topological structure with multiple terminal groups would be advantageous for gene transfection, our group first developed highly branched poly(β-amino ester)s (HPAEs) through the establishment of an "A2+B3+C2" Michael addition platform in 2015 [23]. To date, more than 70 HPAEs with distinct chemical compositions and branched structures have been developed. Moreover, various modification strategies have also been proposed to further enhance the gene transfection efficiency and safety profile of HPAEs [24–29]. Results show that HPAEs with a relatively low or intermediate branching degree are more favorable for gene transfection. Notably, the

* Corresponding authors.
E-mail addresses: dezhong.zhou@xjtu.edu.cn (D. Zhou), lincguo@100biotech.com (L. Guo), 598725073@qq.com (Y. Mao).

https://doi.org/10.1016/j.cclet.2024.109737
1001-8417/

optimized HPAEs can efficiently transfect a wide range of cells, including primary cells, stem cells, and astrocytes, with transfection efficiency even up to 98%. In particular, high-performing HPAEs can deliver plasmids encoding nerve growth factor (NGF) to promote neurite formation and outgrowth in PC12 cells. Recently, it has also been demonstrated that multicyclic structure and the branching unit distribution can significantly affect the gene transfection efficiency of poly(β-amino ester)s [19,29]. *In vivo*, optimal HPAEs effectively delivered COL7A1 to restore high-level and long-term expression of collagen VII in recessive dystrophic epidermolysis bullosa (RDEB) mouse models [24,30].

Despite significant progress, the gene transfection capability of HPAEs derived from the 3D branched structure remains largely untapped. During the "A2+B3+C2" Michael addition strategy, C2-type diacrylates and B3-type triacrylates react simultaneously with A2-type amines, leading to the formation of tertiary amines at the branching sites, along with inactive A2-type secondary amines in the peripheries. A second endcapping amine (ECA) is then added to consume the residual acrylates and generate ECA-type secondary/tertiary amines in the peripheries simultaneously [31]. However, the A2-type secondary amines do not significantly contribute to the gene transfection capability like ECA-type secondary/tertiary amines do [32]. While controlling the feed ratio of A2/B3/C2 monomers can reduce the number of A2-type secondary amines, there is still a lack of research on converting the A2-type secondary amines to ECA-type secondary/tertiary amines *in-situ* to maximize the gene transfection capability of HPAEs. In this study, we aim to investigate the possibility of enhancing the gene transfection efficiency of HPAEs by converting the peripheral A2-type secondary amine groups to ECA-type secondary/tertiary amines *in-situ*. Initially, three HPAEs with varying molecular weights were synthesized. Subsequently, through sequential modification, the peripheral A2-type secondary amine was transformed into ECA-type secondary/tertiary amine *in-situ* (Fig. 1). The physiological properties and gene transfection performance of HPAEs with ECA-type secondary/tertiary amines (HPAE-X-M) were then compared to those with A2-type secondary amine (HPAE-X-B).

4-Amino-1-butanol (S4), trimethylolpropane triacrylate (TMPTA), and bisphenol A ethoxylate diacrylate (BEDA) were utilized as the A2, B3, and C2-type monomers, respectively. Three HPAE base polymers, namely HPAE-1, HPAE-2, and HPAE-3, with weight average molecular weights (M_w) of approximately 4400, 9800, and 21,000 Da, were synthesized using the "A2+B3+C2" Michael addition strategy (Table S1 and Figs. S1–S4 in Supporting information). To promote the formation of A2-type secondary amine (S4), the stoichiometric ratio of A2:B3:C2 was set as 2.8:1.2:1. This ensured an equal probability of generating A2-type secondary amine and C2-type vinyl groups at the peripheries of HPAE base polymers. Next, HPAE-1, HPAE-2, and HPAE-3 were divided into two portions. One portion was directly endcapped with 3-morpholinopropylamine (MPA) to consume the residual vinyl groups derived from BEDA, resulting in HPAE-1-B, HPAE-2-B, and HPAE-3-B with M_w of 6100, 11,800 and 22,700 Da (Table 1, Tables S2 and S3 in Supporting information). In contrast, the other half of HPAE-1, HPAE-2, and HPAE-3 were first reacted with BEDA to convert all the A2-type secondary amines at the periphery to C2-type vinyl groups. Subsequently, MPA was used to further endcap the polymers, consuming all the vinyl groups and converting them into ECA-type secondary/tertiary amines, yielding HPAE-1-M, HPAE-2-M, and HPAE-3-M. Therefore, HPAE-X-B has a similar topological structure and chemical composition to HPAE-X-M, but with a higher content of ECA-type secondary/tertiary amines. Gel permeation chromatography (GPC) revealed a slight increase in the molecular weight of HPAE-1-M, HPAE-2-M, and HPAE-3-M (*i.e.*, 6500, 12,500 and 25,800 Da, respectively) compared to HPAE-X-B (Table 1 and Figs. S5–S10 in Supporting information). Moreover, the chemical composition of the polymers was confirmed using proton nuclear magnetic resonance (^{1}H NMR) (Fig. S11 in Supporting information).

Table 1
Molecular weight and distribution of different HPAE-X-B and HPAE-X-M.[a]

HPAEs	M_n (Da)	M_w (Da)	$Đ$
HPAE-1-B	4900	6100	1.25
HPAE-1-M	5200	6500	1.25
HPAE-2-B	7200	11,800	1.63
HPAE-2-M	7400	12,500	1.68
HPAE-3-B	9600	22,700	2.36
HPAE-3-M	10,400	25,800	2.48

[a] M_n, M_w and $Đ$ were determined by GPC equipped with a refractive index (RI) detector.

The influence of peripheral secondary/tertiary amine groups on the physiological properties of HPAE-X-M and HPAE-X-B was first examined. To confirm the DNA condensation ability of different HPAE-X-M and HPAE-X-B, agarose gel electrophoresis was conducted. At the tested HPAE/DNA weight/weight (w/w) ratios of 5:1

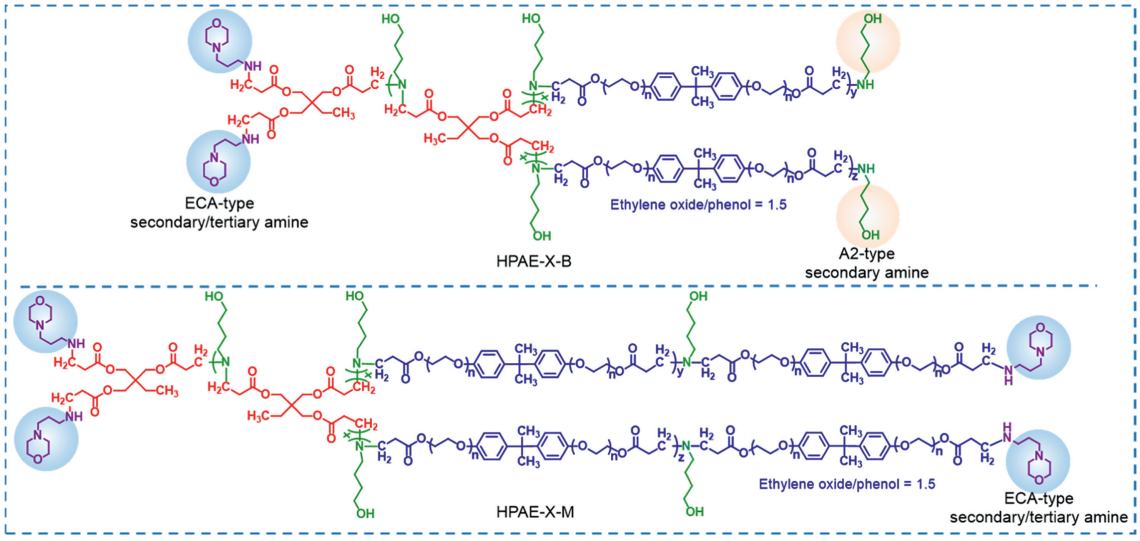

Fig. 1. Schematic structures of HPAE-X-B and HPAE-X-M with varying terminal amine groups.

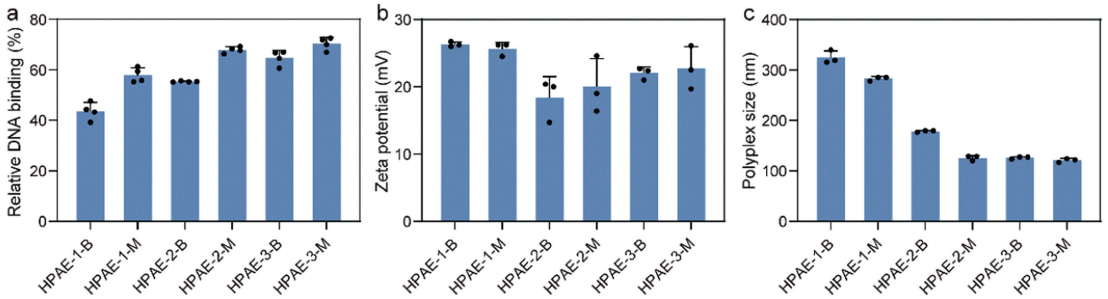

Fig. 2. (a) Relative DNA binding affinity of HPAE-X-B and HPAE-X-M at the w/w ratio of 5:1. (b) The zeta potential of HPAE-X-B/DNA and HPAE-X-M/DNA polyplexes at the w/w ratio of 5:1. (c) The size of HPAE-X-B/DNA and HPAE-X-M/DNA polyplexes at the w/w ratio of 5:1.

and 10:1, all the HPAE-X-M and HPAE-X-B effectively condensed DNA without any evident DNA shift bands (Fig. S12 in Supporting information). Picogreen assay shows that at a HPAE/DNA w/w ratio of 5:1, HPAE-1-B demonstrated relatively low DNA binding affinity, reaching only 43.6% (Fig. 2a). Conversely, HPAE-1-M exhibited higher DNA binding affinity, reaching 58.0%. Similar trends were observed with HPAE-2-B/HPAE-2-M and HPAE-3-B/HPAE-3-M, resulting in increased DNA binding affinities of 12.6% and 5.6%, respectively. In addition, an increase in M_w led to an increase in the DNA binding affinity for both HPAE-X-B and HPAE-X-M, ranging from approximately 43.6% to 70.4%, suggesting that M_w also significantly impacts the DNA binding affinity. Due to their strong DNA binding affinity, all HPAEs were capable of condensing DNA into polyplexes. HPAE-1-B/DNA and HPAE-1-M/DNA polyplexes exhibited similar zeta potentials of approximately +26.0 mV (Fig. 2b). In contrast, HPAE-2-M/DNA and HPAE-3-M/DNA polyplexes displayed zeta potentials 1.6 mV and 0.7 mV slightly higher than those of HPAE-2-B/DNA and HPAE-3-B/DNA polyplexes, respectively. Moreover, HPAE-X-M/DNA polyplexes exhibited smaller sizes compared to their HPAE-X-B/DNA counterparts. At the w/w ratio of 5:1, the sizes of HPAE-X-M/DNA polyplexes were 283.1, 125.9, and 121.3 nm, respectively, while their HPAE-X-B/DNA counterparts measured 324.8, 178.6, and 126.4 nm (Fig. 2c). The increase in M_w resulted in smaller polyplex sizes, possibly due to enhanced DNA binding affinity leading to more compact polyplexes. In addition, the morphologies of the polyplexes were observed using transmission electron microscopy (TEM). Both HPAE-3-B/DNA and HPAE-3-M/DNA polyplexes exhibit similar spherical morphology (Fig. S13 in Supporting information). Effective cellular uptake of polyplexes is crucial for successful gene transfection. Therefore, the cellular uptake of HPAE-3-B/DNA and HPAE-3-M/DNA polyplexes was investigated. As illustrated in Fig. S14 (Supporting information), a high cellular uptake efficiency was observed for both types of polyplexes after 4 h of incubation. These findings collectively indicate that the augmentation of peripheral ECA-type secondary/tertiary amines indeed enhance the interaction between HPAEs and DNA, which is advantageous for gene transfection.

The gene transfection capability of HPAE-X-B and HPAE-X-M was further assessed. Typically, the optimal w/w ratio for effective gene transfection using HPAE-based polymers falls within the range of 10:1 to 60:1. Therefore, w/w ratios of 20:1 and 40:1 were initially employed to screen the transfection conditions for HPAE-X-B and HPAE-X-M. Using a green fluorescence protein (GFP)-encoding plasmid as the reporter gene and branched polyethyleneimine with a M_w of 25,000 Da (PEI 25k) and jetPEI as positive controls, the percentage of GFP-positive was observed 48 h post-transfection. As shown in Fig. S15 (Supporting information), except for HPAE-3-M at the w/w ratio of 20:1, almost no noticeable GFP-positive cells were observed. PEI 25k and jetPEI also did not yield significant GFP expression under their standard transfection protocols, indicating the difficult-to-transfect nature of UM-UC-3. Further analysis revealed high cytotoxicity at these w/w ratios. Consequently, reduced w/w ratios of 5:1 and 10:1 were tested. Encouragingly, a high percentage of GFP expression was observed for HPAE-3-B and HPAE-3-M (Fig. 3a and Fig. S16 in Supporting information). Flow cytometry analysis demonstrated that PEI 25k and jetPEI achieved approximately 8.9% and 6.82% GFP expression, respectively (Fig. 3b). While HPAE-1-B and HPAE-1-M only achieved 7.4% and 10.5% transfection efficiency, HPAE-2-B achieved high GFP expression of 25.1% and 29.9% at the two w/w ratios. Notably, HPAE-2-M resulted in even higher GFP expression of 44.1% and 39.5%, as evidenced by the right shift of the histogram (Fig. 3c). Furthermore, the mean fluorescence intensity (MFI) of individual cells after transfection also substantially increased (Fig. 3d). Remarkably, HPAE-3-M achieved gene transfection efficiency as high as 57.4% at the w/w ratio of 10:1. Cell viability tests further demonstrated that all HPAEs did not exhibit significant cytotoxicity. Even at the w/w ratio of 10:1, HPAE-3-M maintained a cell viability of approximately 80.8% (Fig. S17 in Supporting information).

To further evaluate the gene transfection capability of HPAE-X-B and HPAE-X-M in bladder epithelial cells, SV-HUC-1 were employed. At the optimized w/w ratios of 5:1 and 10:1, strong GFP expression was observed 48 h post-transfection with all HPAEs (Fig. 4a and Fig. S18 in Supporting information). Interestingly, similar to UM-UC-3 cells, SV-HUC-1 cells also present challenges in transfection. The leading commercial gene transfection reagents, PEI 25k and jetPEI, only achieved low percentages of GFP expression (Fig. 4b). HPAE-1-B and HPAE-1-M also exhibited relatively weak gene transfection capabilities, possibly due to their low M_w. However, as the M_w increased, significantly stronger gene transfection efficiency was achieved. Interestingly, a lower w/w ratio was found to be more favorable for transfection. At the w/w ratio of 5:1, HPAE-2-B and HPAE-3-B exhibited 21.2% and 32.0% gene transfection efficiency, respectively, compared to 15.0% and 27.2% at the w/w ratio of 10:1. Excitingly, regardless of the w/w ratios, HPAE-2-M and HPAE-3-M consistently demonstrated stronger gene transfection capabilities than HPAE-2-B and HPAE-3-B (Fig. 4c). Notably, HPAE-3-M achieved 40.4% transfection efficiency at the w/w ratio of 5:1, which is 3.1-fold and 3.4-fold higher compared to PEI 25k and jetPEI, respectively. The MFI analysis of SV-HUC-1 cells after transfection showed similar trends to the percentage of GFP-positive cells, with the highest MFI achieved by HPAE-2-M at the w/w ratio of 5:1 (Fig. 4d). Cell viability tests indicated that although high cytotoxicity was observed at the w/w ratio of 10:1, up to 102% and 115% of cells remained viable at the optimal w/w ratio of 5:1 (Fig. S19 in Supporting information). These results clearly demonstrate that the conversion of A2-type secondary amines to ECA-type secondary/tertiary amines enhances the gene transfection capability of HPAEs. Moreover, in certain cases, lower w/w ratios (*i.e.*, 5) are even more favorable for achieving high gene transfection efficiency while ensuring a satisfactory safety profile. It is worth noting that bladder epithelial cells are particularly challeng-

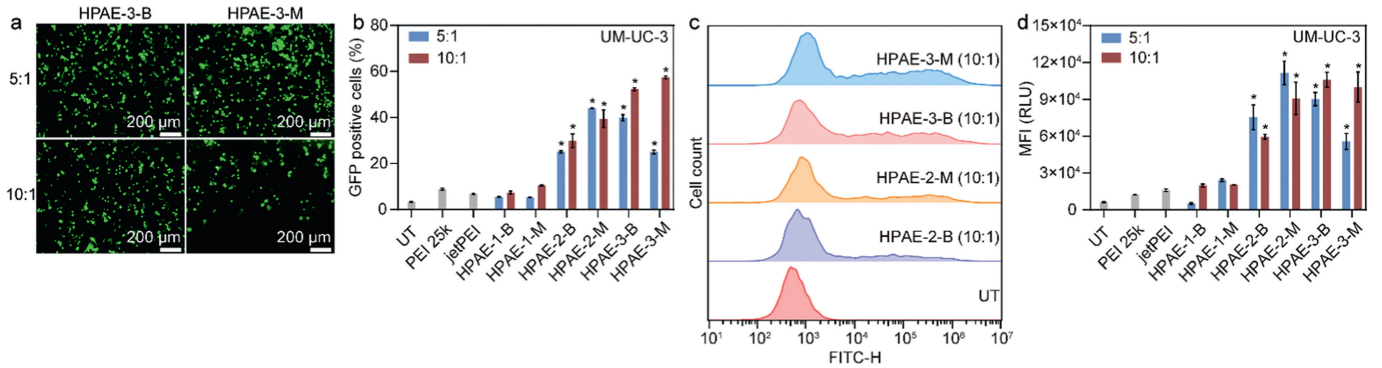

Fig. 3. (a) Fluorescence images of UM-UC-3 bladder epithelial cells after transfection with HPAE-3-B and HPAE-3-M. Scale bars: 200 μm. (b) Percentage of GFP-positive UM-UC-3 cells measured by flow cytometry. Data are presented as mean ± SD ($n = 3$), $^*P < 0.05$. (c) Histogram distribution of flow cytometry results. (d) MFI of UM-UC-3 cells measured by flow cytometry. Data are presented as mean ± SD ($n = 3$), $^*P < 0.05$.

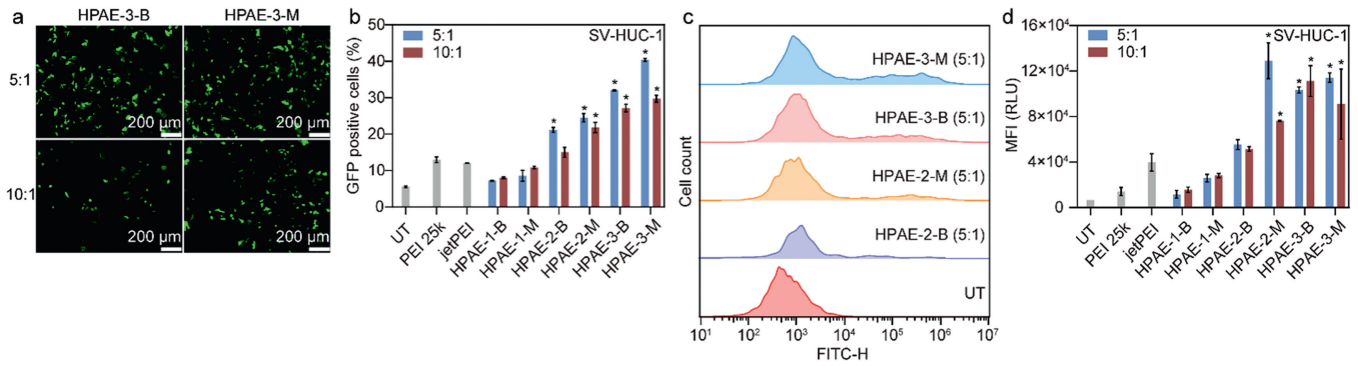

Fig. 4. (a) Fluorescence images of SV-HUC-1 bladder epithelial cells after transfection with HPAE-3-B and HPAE-3-M. Scale bars: 200 μm. (b) Percentage of GFP-positive UM-UC-3 cells measured by flow cytometry. Data are presented as mean ± SD ($n = 3$), $^*P < 0.05$. (c) Histogram distribution of flow cytometry results. (d) MFI of SV-HUC-1 cells measured by flow cytometry. Data are presented as mean ± SD ($n = 3$), $^*P < 0.05$.

ing to transfect, as evidenced by the low efficiency of commercial gene transfection reagents. The high transfection potency of HPAE-X-M holds great potential for applications in the treatment of bladder-related diseases.

In conclusion, this study presents a novel strategy to enhance the gene transfection capability of HPAEs by converting A2-type secondary peripheral amines to ECA-type secondary/tertiary amines. Instead of complex optimization of their topological structure and chemical composition, it successfully demonstrated that increasing the content of ECA-type secondary/tertiary amines improves various physiological properties of HPAEs, including DNA binding affinity, zeta potential, and size of formulated polyplexes, ultimately leading to enhanced gene transfection efficiency. Importantly, the achieved high gene transfection efficiency allows for further reduction of the w/w ratios, thus enhancing the safety of HPAEs in gene therapy applications. The remarkable gene transfection efficiency of HPAE-X-M observed in UM-UC-3 and SV-HUC-1 cells highlights their promising potential for bladder-related disorders.

Declaration of competing interest

The authors declare that they have no known competing financial interests or personal relationships that could have appeared to influence the work reported in this paper.

Acknowledgments

This work was funded by the National Natural Science Foundation of China (NSFC, No. 51903202), the Key R&D Program of Shaanxi Province (No. 2020GXLH-Y-016), the Natural Science Foundation of Shaanxi Province (No. 2020JM-055), the Fundamental Research Funds for the Central Universities (No. xtr042019020) and the Young Talents Support Plan of Xi'an Jiaotong University (No. HG6J002).

Supplementary materials

Supplementary material associated with this article can be found, in the online version, at doi:10.1016/j.cclet.2024.109737.

References

[1] R. SoRelle, Circulation 101 (2000) e9001.
[2] T.L. Roth, A. Marson, Annu. Rev. Pathol. 24 (2021) 145–166.
[3] D. Castanotto, J.J. Rossi, Nature 457 (2009) 426–433.
[4] D.M. Markusic, A.T. Martino, C.D. Porada, et al., Mol. Ther. 28 (2020) 691–692.
[5] C.T. Charlesworth, I. Hsu, A.C. Wilkinson, et al., Nat. Rev. Immunol. 22 (2022) 719–733.
[6] Y. Zou, X. Sun, Q. Yang, et al., Sci. Adv. 8 (2022) eabm8011.
[7] Q. Bi, X. Song, A. Hu, et al., Chin. Chem. Lett. 31 (2020) 3041–3046.
[8] J. Wang, H. Wang, H. Cui, et al., Chin. Chem. Lett. 31 (2020) 3143–3148.
[9] Y. Zhang, L. Wang, J. Wang, S. Xin, X. Sheng, Chin. Chem. Lett. 32 (2021) 1902–1906.
[10] H. Khan, A. Khan, Y. Liu, et al., Chin. Chem. Lett. 30 (2019) 2201–2204.
[11] Q. Zhang, G. Kuang, W. Li, et al., Nanomicro. Lett. 8 (2023) 44–76.
[12] Y. Wang, C. Li, L. Du, Y. Liu, Chin. Chem. Lett. 31 (2020) 275–280.
[13] D.X. Yin, M.J. Zhang, J.X. Chen, Y.Y. Huang, D.H. Liang, Chin. Chem. Lett. 32 (2021) 1731–1736.
[14] J.T. Bulcha, Y. Wang, H. Ma, et al., Signal Transduct. Target. Ther. 6 (2021) 53.
[15] V. Picanço-Castro, C.G. Pereira, D.T. Covas, et al., Nat. Biotechnol. 38 (2020) 151–157.
[16] J.J. Green, R. Langer, D.G. Anderson, Acc. Chem. Res. 41 (2008) 749–759.
[17] D.G. Anderson, D.M. Lynn, R. Langer, Angew. Chem. 115 (2003) 3261–3266.
[18] D.M. Lynn, M.M. Amiji, R. Langer, Angew. Chem. Int. Ed. 40 (2001) 1707–1710.
[19] Y. Li, X. Wang, Z. He, et al., J. Am. Chem. Soc. 145 (2023) 17187–17200.
[20] D.M. Lynn, R. Langer, J. Am. Chem. Soc. 122 (2000) 10761–10768.

[21] A.A. Eltoukhy, D. Chen, C.A. Alabi, R. Langer, D.G. Anderson, Adv. Mater. 25 (2013) 1487–1493.
[22] U.C. Palmiero, J.C. Kaczmarek, O.S. Fenton, D.G. Anderson, Adv. Mater. 25 (2018) 1800249.
[23] L. Cutlar, D. Zhou, Y. Gao, et al., Biomacromolecules 16 (2015) 2609–2617.
[24] D. Zhou, L. Cutlar, Y. Gao, et al., Sci. Adv. 2 (2016) e1600102.
[25] M. Zeng, Q. Xu, D. Zhou, et al., Adv. Drug Deliv. Rev. 176 (2021) 113842.
[26] D. Zhou, Y. Gao, A. Aied, et al., J. Control. Release 244 (2016) 336–346.
[27] J. Shi, Y. Zhang, B. Ma, et al., ACS App. Mater. Interfaces 36 (2023) 42130–42138.
[28] Q. Li, L. Sun, X. Huang, et al., ACS Macro Lett. 5 (2022) 636–642.
[29] Y. Li, Z. He, X. Wang, et al., ACS Macro Lett. 12 (2023) 780–786.
[30] S. Liu, Y. Gao, D. Zhou, et al., Nat. Commun. 1 (2019) 3307.
[31] J.J. Green, J. Shi, E. Chiu, et al., Bioconjugate Chem. 17 (2006) 1162–1169.
[32] G.T. Zugates, W. Peng, A. Zumbuehl, et al., Mol. Ther. 7 (2007) 1306–1312.